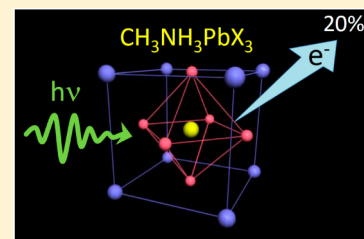


Organometal Perovskite Light Absorbers Toward a 20% Efficiency Low-Cost Solid-State Mesoscopic Solar Cell

Nam-Gyu Park*

School of Chemical Engineering and Department of Energy Science, Sungkyunkwan University, Suwon 440-746, Republic of Korea

ABSTRACT: Recently, perovskite $\text{CH}_3\text{NH}_3\text{PbI}_3$ sensitizer has attracted great attention due to its superb light-harvesting characteristics. Organometallic or organic materials were mostly used as sensitizers for solid-state dye-sensitized solar cells at early stages. Inorganic nanocrystals have lately received attention as light harvesters due to their high light-absorbing properties. Metal chalcogenides have been investigated with solid-state dye-sensitized solar cells; however, the best power conversion efficiency was reported to be around 6%. $\text{CH}_3\text{NH}_3\text{PbX}_3$ ($X = \text{Cl}, \text{Br}, \text{or I}$) perovskite sensitizer made a breakthrough in solid-state mesoscopic solar cells, where the first record efficiency of around 10% was reported in 2012 using submicrometer-thick TiO_2 film sensitized with $\text{CH}_3\text{NH}_3\text{PbI}_3$. A rapid increase in efficiency approaching 14% followed shortly. In this Perspective, recent progress in perovskite-sensitized solid-state mesoscopic solar cells is reviewed. On the basis of the recent achievements, a power conversion efficiency as high as 20% is expected based on optimized perovskite-based solid-state solar cells.



Progress in Solid-State Dye-Sensitized Solar Cells. Since the first report of low-cost dye-sensitized solar cells (DSSCs) in 1991,¹ a tremendous number of research papers have spouted during last two decades. As a consequence of the DSSC-related research efforts, the beginning efficiency of around 8% was improved to over 12%.² High efficiency more than 12% was obtained using a 10 μm mesoporous TiO_2 film sensitized with organic dyes and a cobalt-based redox electrolyte. Meanwhile, solid-state DSSC was introduced in 1998,³ where the liquid electrolyte was replaced by organic hole-transport material (HTM) such as 2,2',7,7'-tetrakis(*N,N*-*p*-dimethoxy-phenylamino)-9,9'-spirobifluorene (spiro-MeOTAD). A maximum incident photon-to-electron conversion efficiency (IPCE) as high as 33% was achieved using spiro-MeOTAD. However, the power conversion efficiency (PCE) under one sun intensity (100 mW/cm^2) was as low as 1%. Thus, no spotlight on solid-state DSSCs was received at early stages.

Recently, the perovskite $\text{CH}_3\text{NH}_3\text{PbI}_3$ sensitizer has attracted great attention due to its superb light-harvesting characteristics.

The low efficiency that originated from charge recombination across the interface of the TiO_2 /spiro-MeOTAD heterojunction was overcome by incorporating 4-*tert*-butylpyridine (*t*BP) and lithium bis(trifluoromethanesulfonyl)imide (LiTFSI), $\text{Li}[\text{CF}_3\text{SO}_2]_2\text{N}$, in spiro-MeOTAD, which resulted in a PCE of 2.56% at AM 1.5 one sun condition.⁴ The photoanode of the 2.56% efficiency device was composed of a $\sim 2.5 \mu\text{m}$ thick mesoporous TiO_2 film sensitized with $(\text{Bu}_4\text{N})_2[\text{Ru}(\text{dcbpyH})_2(\text{NCS})_2]$ dye (coded N719). Compared to the bare spiro-MeOTAD, it

was found from nanosecond laser spectroscopic study that the presence of LiTFSI and *t*BP in spiro-MeOTAD inhibited the interface charge carrier recombination.⁴ In solid-state DSSCs, an increase in TiO_2 film thickness may be restricted because of the limited mean free path of hole transport in spiro-MeOTAD. Therefore, a film thickness of about 2 μm has been proposed to be optimal, which was, however, too thin to maximize light harvesting. A little improvement of PCE to 3.2% was achieved by increasing the optical absorption from mixing silver ions in N719 dye solution.⁵ No significant progress was made until replacement of the N719 dye with amphiphilic ruthenium dye (Z907)⁶ or pure organic indoline dye (D102),⁷ where both Z907 and D102 showed PCEs of around 4%. For the Z907 case, unlike N719, it turned out that the silver ion no longer had a positive effect. Although the absorption onset wavelength of D102 (600 nm in ethanol) was shorter than that of N719 (710 nm in ethanol), higher performance with D102 was due to a higher molar extinction coefficient ($5.6 \times 10^4 \text{ L mol}^{-1} \text{ cm}^{-1}$ at 491 nm)⁷ compared to that of N719 ($\sim 1.6 \times 10^4 \text{ L mol}^{-1} \text{ cm}^{-1}$ at 530 nm), which underlines that high absorption coefficient sensitizers are beneficial to a thinner photoanode such as a solid-state DSSC. Learning from the high absorption coefficient heteroleptic ruthenium complex. Compared to Z907, a 2-fold higher absorption coefficient C104 dye was developed, which demonstrated a PCE of 4.6% with long-term stability (photo-voltaic parameters retained more than 80% of the initial value after 1000 h of light soaking).⁸ Organic dyes with strong absorption characteristics were also developed in parallel to improve further photovoltaic performance of solid-state DSSCs. As a result, C220 organic dye with a molar absorption coefficient of

Received: April 27, 2013

Accepted: July 11, 2013

Published: July 11, 2013



$5.5 \times 10^4 \text{ M}^{-1} \text{ cm}^{-1}$ at 555 nm (5 times higher than that of Z907) demonstrated a PCE of more than 6%.⁹ Although spiro-MeOTAD is proposed as a useful hole-transporting material, it suffers from low conductivity in its pristine form.^{10,11} A remarkable improvement in PCE (7.2%) was achieved by increasing the conductivity of spiro-MeOTAD via doping technology, where more than 1 order of magnitude increase in conductivity was realized by 1% doping with tris(2-(1H-pyrazol-1-yl)pyridine)cobalt(III) (coded FK102).¹²

Meanwhile, conjugate polymers have been simultaneously studied as alternatives to spiro-MeOTAD because of high conductivity and thermal stability. Polyaniline¹³ and polypyrrole¹⁴ were studied for solid-state DSSCs at first. However, PCEs were less than 1%. Poly(3-alkylthiophene)s such as poly(3-hexylthiophene) (P3HT) and poly(3-octylthiophene) (P3OT) were tried, but their initial performances were poor (<1%),^{15–17} which was ascribed to inefficient pore filling of polymer HTMs into mesoporous TiO_2 film and polymer– TiO_2 interfaces, associated with charge separation and collection.^{18,19} As was the case with spiro-MeOTAD, the problem in P3HT bearing solid-state DSSCs was solved by addition of lithium salts and *t*BP. The D102-sensitized TiO_2 /P3HT device demonstrated an improved PCE of 2.63% via LITFSI and *t*BP treatment.²⁰ Low efficiency for the P3HT-based cell without additives was because electron transfer from the excited dye to TiO_2 was hindered by forster resonant energy transfer (FRET) from D102 to P3HT, as confirmed by spectral overlap between D102 photoluminescence (PL) and P3HT absorption, while the presence of additive reduced the overlap by a red shift of the dye PL and accelerated electron transfer to TiO_2 as well.²¹ A further improvement of PCE to 3.2% was achieved by infiltration of P3HT into the vertically aligned TiO_2 nanotubes sensitized with squaraine dye (SQ-1).²²

Quantum leap in solid-state DSSCs did not happen until nanoscale inorganic semiconductors were applied as light harvesters.

Quantum leap in solid-state DSSCs did not happen until nanoscale inorganic semiconductors were applied as light harvesters. When P3HT-based solid-state DSSCs employed the Sb_2S_3 nanocrystal as a light harvester, a PCE of about 5% was achieved.²³ Replacement of P3HT with a modified poly(alkylthiophene), poly(2,6-(4,4-bis-(2-ethylhexyl)-4H-cyclopenta[2,1-*b*;3,4-*b'*]dithiophene)-*alt*-4,7(2,1,3-benzothiadiazole) (PCPDTBT), improved further the PCE to 6.3%.^{24,25} Breakthrough for the spiro-MeOTAD-based solid-state DSSC was made in 2012 using organometal halides $\text{CH}_3\text{NH}_3\text{PbI}_3$ having perovskite structure, in which submicrometer-thick mesoporous TiO_2 film adsorbed with perovskite $\text{CH}_3\text{NH}_3\text{PbI}_3$ nanocrystals exhibited a PCE of 9.7% under the simulated AM1.5G one sun illumination.²⁶ The device stored for 500 h in air at room temperature without encapsulation retained its photovoltaic performance. High-efficiency solid-state technology was developed almost at the same period of time using a $\text{CH}_3\text{NH}_3\text{PbI}_2\text{Cl}$ perovskite, where a PCE of more than 10% was achieved when the perovskite adsorbed on Al_2O_3 was in contact with spiro-MeOTAD.²⁷ Al_2O_3 used in this device acted simply as a scaffold layer, not as an electron-accepting layer. The remarkable

achievement from perovskite materials promises further breakthroughs in this field of study. The progress in solid-state DSSCs is depicted in Figure 1. As can be seen in Figure 1,

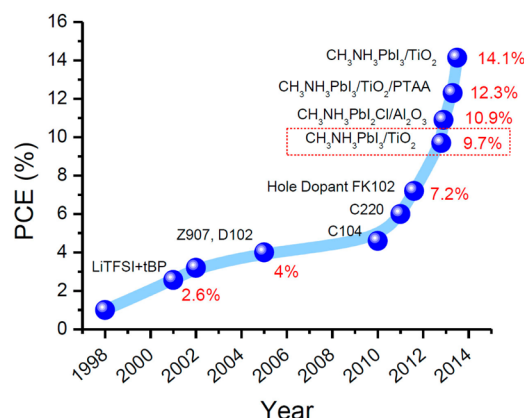


Figure 1. Progress in solid-state DSSCs. A PCE of less than 1% was first reported in 1998 using spiro-MeOTAD in combination with N719. Addition of LITFSI and *t*BP in spiro-MeOTAD improved the PCE to 2.6%. A change from N719 to organic dye D102 enhanced the PCE to 4%. More than 7% was achieved by using hole dopant FK102. A breakthrough in solid-state DSSC technology was made in 2012 by introducing organometal perovskite sensitizers $\text{CH}_3\text{NH}_3\text{PbX}_3$ (X = halides), where a $\text{CH}_3\text{NH}_3\text{PbI}_3$ -sensitized submicrometer mesoporous TiO_2 layer showed 9.7% and $\text{CH}_3\text{NH}_3\text{PbI}_2\text{Cl}$ on the scaffold Al_2O_3 layer demonstrated 10.9%. In a very short period from August 2012 to March 2013, a PCE as high as 14.1% was achieved from the perovskite sensitizer.

no noticeable achievement was made from 1998 to 2011, but a very steep increase in progress happened in a very short period in 2012 thanks to the development of perovskite sensitizer. Further improvement in PCE was achieved in 2013, where 12.3% was reported using a perovskite sensitizer and poly-(triarylamine) (PTAA) HTM,²⁸ and a higher efficiency of 14.1% was newly added in the research cell efficiency records provided by the National Renewable Energy Laboratory (NREL) (<http://www.nrel.gov/ncpv/>).

Fabrication of Solid-State DSSCs. The solid-state DSSC structure is “pseudo pin junction” type, where an intrinsic (i) light harvester adsorbed on an n-type (n) TiO_2 surface is in contact with a p-type (p) HTM. Figure 2 shows a real device along with

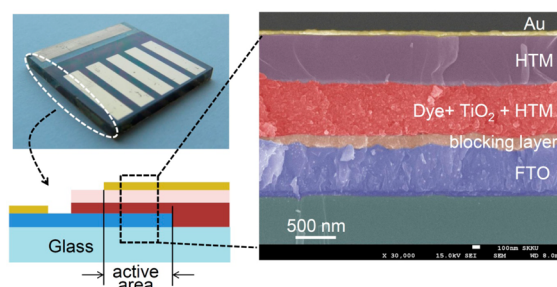


Figure 2. Solid-state DSSC structure showing (left) a real device with the cross-sectional structure and (right) the cross-sectional SEM image.

the cross-sectional layer structure, where a compact thin layer, called the “blocking layer”, forms first on a transparent conductive oxide (TCO) substrate to protect recombination

of the electron in TCO and the hole in HTM. A metal layer such as gold or silver is deposited on top of the HTM layer, in which the work function of the metal should be considered in order to transfer the hole from the HTM layer. Because electrons are collected at TCO, the TCO substrate with the TiO₂ film is a photoanode (minus electrode), and the metal layer on HTM is the cathode (plus electrode).

The fabrication process is as follows. First, a compact TiO₂ blocking layer is deposited on a TCO substrate, where fluorine-doped tin oxide (FTO) has been usually used for TCO because the high haze surface of FTO provides a strong adhesion with the nanoparticle TiO₂ film. This is an important step because the role of the compact layer is to protect direct contact between the FTO and HTM. Once the compact layer forms, nanoparticle TiO₂ paste is deposited on the compact layer covered FTO substrate and annealed at around 500–550 °C to have a mesoporous film. In this process, the porosity and thickness should be carefully controlled because porosity and thickness are related to the pore filling and conductivity of HTM. Sensitizers are then adsorbed on the annealed TiO₂ film, which is followed by spin-coating the HTM solution. During spin-coating, HTM is infiltrated into the pores of the TiO₂ film. The degree of infiltration is related to the pore filling fraction (PFF) that was found to have a significant effect on photovoltaic performance.^{29–31} PFF can be estimated by optical reflectometry.³² Finally, the metal electrode is formed on the HTM layer using a thermal evaporator.

In a very short period from August 2012 to March 2013, a power conversion efficiency as high as 14.1% was achieved from the perovskite sensitizer.

Materials for Solid-State DSSCs. As mentioned previously, materials comprising solid-state DSSCs are the (i) blocking layer, (ii) oxide film, (iii) sensitizer, (iv) HTM, and (v) metal electrode. Here, the role of each material and factors affecting the photovoltaic performance of DSSCs are investigated.

Blocking Layer. In liquid-type DSSCs, the presence of a blocking layer was reported to improve slightly the photovoltaic performance compared to the device without a blocking layer,³³ which indicates that the blocking layer is not a major concern when designing the liquid-electrolyte-contained DSSC. However, the blocking layer is of particular importance and thus requisite for solid-state DSSCs. It was reported that the blocking layer played an important role in blocking the flow of electrons from the FTO to HTM or holes from the HTM to FTO, which was confirmed by rectifying the behavior of the blocking layer³⁴ due to the Schottky barrier built in the junction between the FTO and the compact thin TiO₂ layer.³⁵ The thickness of the blocking layer can have an influence on the photovoltaic performance. It was proposed that the optimal thickness of the blocking layer prepared by spray pyrolysis was about 120–160 nm.³⁶ However, the spin-coating method led to an optimal thickness of about 80–100 nm.²⁶ Therefore, the blocking layer morphology and thickness should be carefully controlled depending on the deposition methods. In addition, a thicker blocking layer should be avoided because the fill factor and charge collection may be lowered by the increased resistance. The proposed thicknesses seem to be still thick

and therefore must be further optimized. A method for a thinner blocking layer (40–70 nm thick) was recently proposed, where a diblock copolymer was mixed with titanium isopropoxide.³⁷

Mesoscopic Oxide Layer. The oxide layer plays a role in accepting the excited electrons from the sensitizer. For this purpose, the conduction band of the oxide is lower than the excited state of the sensitizer in order to inject the photoexcited electrons from the sensitizer to the oxide layer. TiO₂ has been known to be the best material among the studied oxides such as ZnO and SnO₂ for both liquid-type and solid-state DSSCs. For solid-state DSSCs, the pore size of TiO₂ is of particular importance because HTM should be completely infiltrated into the entire TiO₂ matrix to form a solid HTM layer. In the case of an iodide-based liquid-electrolyte-contained DSSC, larger pores are not necessarily required because of the small size of iodide and tri-iodide. However, even in the case of the liquid electrolyte system, the importance of pore size was emphasized when the larger cobalt bipyridine redox shuttle was employed.³⁸ The pore size and/or porosity of the nanocrystalline TiO₂ film affect the degree of PFF of the HTM. The dependence of pore filling of the HTM on photovoltaic performance was investigated for the case of spiro-MeOTAD, where the size of the used TiO₂ particle was around 20 nm.³¹ The 3-fold increase in PCE was observed by increasing the PFF from 26 to 65% due to a significant increase in the photocurrent density and voltage, which was related to the huge improvement of the hole injection efficiency from about 58 to 95%.³¹ An ordered mesoporous TiO₂ layer using a polymer template was designed to create an ordered bicontinuous semiconducting network.³⁹ A highly ordered pore structure formed by the polymer template method was better for uniform infiltration of organic HTMs and improvement of electron transfer from sensitizers due to the high availability of sub-band-gap states.⁴⁰ Depending on the chemical structure and formula weight of HTMs, the pore size and porosity of the TiO₂ layer should be carefully controlled. Besides TiO₂, SnO₂ was tested for solid-state DSSCs, where the performance of the SnO₂-based cell was inferior to that of the TiO₂-based one due to low voltage.⁴¹

Sensitizers for Solid-State DSSCs. Natural products such as anthocyanine and synthesized compounds such as ruthenium complexes and organic dyes are candidates for sensitizers for solid-state DSSCs. The most studied and efficient organic sensitizers for solid-state DSSCs were Z907 and triphenylamine-bearing organic materials. Apart from organic sensitizers, inorganic materials may be prime candidates for solid-state DSSCs, which is because inorganic sensitizers usually show a much higher light-absorption property compared to organic molecular sensitizers.^{42,43} Because the overall thickness in solid-state DSSCs is limited to a few micrometers, a high absorption coefficient sensitizer is better for such a thin film solar cell. Inorganic nanocrystals have commonly higher absorption coefficients than organic sensitizers. Because the absorption coefficient is proportional to the molar extinction coefficient and molar concentration or absorption cross section and number density of absorbers according to the Beer–Lambert law, absorption coefficients of solid inorganic nanocrystals are higher than those of molecular organic sensitizers because inorganic nanocrystals can be regarded as a sort of cluster of molecules. Extinction coefficients of colloidal CdX (X = S, Se, and Te) nanocrystals were estimated to be around 10⁵ L mol⁻¹cm⁻¹, 1 order of magnitude higher than that of N719, and they were increased with increasing the size of CdX.⁴⁴ For this reason, inorganic sensitizers such as metal chalcogenides have attracted

much attention in solid-state DSSC research.^{42,43} However, a breakthrough in solid-state DSSCs was made by organo lead halide perovskite-type light harvesters,^{26–28} not by metal chalcogenides so far.

Perovskite $\text{CH}_3\text{NH}_3\text{PbX}_3$ Sensitizers. Perovskite, named after Russian mineralogist Perovski who first characterized the structure, has an ABX_3 formula ($X = \text{halogen or oxygen}$) in general, where A and B cations have 12 and 6 coordinates with X anions, respectively, as confirmed by Helen.⁴⁵ Materials with perovskite structure attracted much attention in the late 1980s and early 1990s due to superconductivity.^{46,47} The stability and distortion of the perovskite structure depend on the ratio of the (A–X) distance to the (B–X) distance, called the tolerance factor (eq 1).⁴⁸

$$t = \frac{(R_A + R_X)}{\sqrt{2}(R_B + R_X)} \quad (1)$$

The cubic phase is stabilized when $(R_A + R_X) = 2^{1/2}(R_B + R_X)$, and distortion of the octahedral $[\text{BX}_6]$ is expected when t deviates from 1. Lead-halide-based perovskite-type crystals have been studied due to their distinctive optical properties that are related to their unique crystal structure. In the organo lead halide perovskite structure, $[\text{PbX}_6]$ octahedra form two- or three-dimensional networks (Figure 3) with the chemical formula of $(\text{RNH}_3)_2\text{PbX}_4$

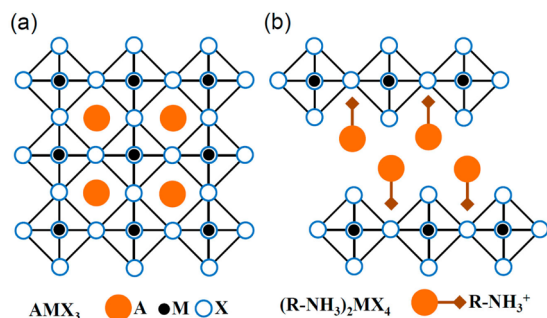


Figure 3. (a) The 3-D cubic AMX_3 perovskite structure with the corner-sharing $[\text{MX}_6]$ octahedral and (b) the 2-D layered structure of the $(\text{R-NH}_3)_2\text{MX}_4$ perovskite.

and $(\text{CH}_3\text{NH}_3)\text{PbX}_3$ ($X = \text{halogen}$), respectively.^{49–52} Regarding the optical property, 3-D lead halide perovskite can be a better candidate than the 2-D one for light harvesting because of the lower band gap energy with lower exciton binding energy (~ 45 meV).⁵³

Perovskite-Sensitized Solar Cells. $\text{CH}_3\text{NH}_3\text{PbX}_3$ ($X = \text{Br, I}$) perovskite was first attempted as light harvester in liquid-based DSSC by Miyasaka's research group in 2009,⁵⁴ where bromide and iodide showed 3.8% and 3.1%, respectively. The band gap of lead bromide was about 2.25 eV, whereas that of lead iodide was around 1.55 eV, as estimated from the threshold values in the IPCE spectra. The efficiencies, however, are much lower than the expected ones, which was due to that fact that the measured photocurrent densities were lower than theoretical ones. The poor efficiency was probably due to nonoptimized conditions such as a diluted precursor solution for perovskite sensitizer coating. More than doubled efficiency (6.5%) was reported by Park's research group in 2011 using $\text{CH}_3\text{NH}_3\text{PbI}_3$ and iodide redox electrolyte.⁵⁵ The band gap energy of $\text{CH}_3\text{NH}_3\text{PbI}_3$ was measured to be about 1.5 eV using UPS and UV–vis spectroscopies. For the given TiO_2 film thickness of $3.6 \mu\text{m}$, the $\text{CH}_3\text{NH}_3\text{PbI}_3$ -sensitized solar cell showed almost two

times higher performance than a conventional N719-sensitized one, which was mainly due to a higher photocurrent density, associated with a higher absorption coefficient. The drawback of the perovskite-sensitized liquid-type DSSC was the instability of the deposited $\text{CH}_3\text{NH}_3\text{PbI}_3$ in liquid electrolyte. Surface protection of the deposited $\text{CH}_3\text{NH}_3\text{PbI}_3$ is thus to be developed to increase its stability in liquid-based DSSCs. The instability issue was actually solved by replacing liquid electrolyte with solid hole conductor spiro-MeOTAD, where an efficiency as high as 9.7% was achieved from a very thin TiO_2 film ($\sim 0.5 \mu\text{m}$) together with excellent long-term stability.²⁶ Hole extraction by spiro-MeOTAD was detected by a femtosecond spectroscopic study. Energy levels in the $\text{TiO}_2/\text{CH}_3\text{NH}_3\text{PbI}_3/\text{spiro-MeOTAD}$ junction are well matched for charge separation (Figure 4).

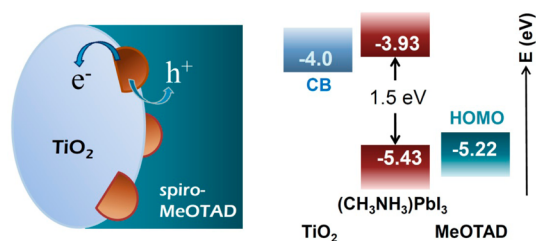


Figure 4. Energy levels of the $\text{TiO}_2/\text{CH}_3\text{NH}_3\text{PbI}_3/\text{spiro-MeOTAD}$ junction showing that the conduction band minimum and valence band maximum of $\text{CH}_3\text{NH}_3\text{PbI}_3$ are well positioned for electron injection into TiO_2 and hole transfer to spiro-MeOTAD, respectively.

Unexpectedly similar charge separation was observed for the $\text{Al}_2\text{O}_3/\text{perovskite}/\text{spiro-MeOTAD}$ system.²⁶ Photovoltaic action was observed from the FTO/TiO_2 blocking layer/ $\text{Al}_2\text{O}_3/\text{perovskite}/\text{spiro-MeOTAD}$, where $\text{CH}_3\text{NH}_3\text{PbI}_2\text{Cl}$ -adsorbed mesoporous Al_2O_3 demonstrated an average efficiency of 5–6% and the highest efficiency of 10.9%.²⁷ It is interesting to see that photoexcited electrons were not injected into Al_2O_3 , which indicates that Al_2O_3 acts as a scaffold layer and $\text{CH}_3\text{NH}_3\text{PbI}_2\text{Cl}$ serves as not only a light harvester but also an electron-transporting layer. To transfer an electron, a continuous structure of the perovskite layer is required. Evidence for the charge-transporting ability in perovskite was shown from the device without the HTM layer, where the $\text{TiO}_2/\text{CH}_3\text{NH}_3\text{PbI}_3$ heterojunction demonstrated a PCE of 5.5%.⁵⁶ In this case, $\text{CH}_3\text{NH}_3\text{PbI}_3$ is likely to play a role in transporting a hole. High photovoltaic performance of a solid-state $\text{CH}_3\text{NH}_3\text{PbI}_3$ -sensitized mesoscopic solar cell was reproduced by Seok's research group,²⁸ where a strikingly high efficiency of 12.3% at one sun illumination was demonstrated using a bromide-incorporated $\text{CH}_3\text{NH}_3\text{PbI}_3$ perovskite and polytriaryamine as a HTM. Besides the iodide-based perovskite sensitizer, $\text{CH}_3\text{NH}_3\text{PbBr}_3$ was also investigated. Although bromide-based perovskite does not seem to be a good candidate because of the larger band gap energy than that of the iodide-based one, a photovoltage as high as 1.3 V may compensate for the loss in photocurrent.⁵⁷ Recently, inorganic semiconducting sensitizers including perovskite were viewed as ‘the next big thing’ in photovoltaics.⁵⁸

Perspective of a Perovskite-Sensitized All-Solid-State Solar Cell. According to the previous report,⁵⁹ a maximum current density of $28 \text{ mA}/\text{cm}^2$ is possible by converting photons in the range of 280–820 nm into electrons, where 820 nm light energy corresponds to a band gap energy of around 1.5 eV. When considering 20% light reflection at the TCO glass substrate, about $22 \text{ mA}/\text{cm}^2$ is a realistic photocurrent density from a

Power conversion efficiency approaching 20% is realistically possible from a solid-state mesoscopic solar cell based on $\text{CH}_3\text{NH}_3\text{PbX}_3$.

1.5 eV band gap material. Therefore, ~17% is a realistic efficiency from $\text{CH}_3\text{NH}_3\text{PbI}_3$ perovskite with a 1.5 eV band gap because a photocurrent density of 22 mA/cm², photovoltage of 1.1 V, and fill factor of 0.7 are achievable. A photovoltage of 1.1 V is expected by considering a driving force of 0.4 eV for electron injection (0.2 eV) and hole extraction (0.2 eV). When using a meso-superstructured structure as proposed by the Henry Snaith group,²⁷ where perovskite acts as not only a light-harvesting material but also as an electron-transporting material, the photovoltage will be determined by the difference between the Fermi energy of the perovskite and the HOMO energy of the HTM. In this case, a photovoltage of more than 1.1 V is possible because the driving force for hole extraction (0.2 V) is only taken into consideration. Because a fill factor of 0.7 was already achieved,²⁸ further improvement such as from 0.7 to 0.75 or more is possible by increasing the shunt resistance and decreasing the series resistance. Application of antireflection or plasmonic technologies is expected to increase the number of photons passed through the conductive substrate, which improves the photocurrent density more than 22 mA/cm². For instance, reduction of the light reflection fraction from 20 to 15% leads to a photocurrent density of about 24 mA/cm². Therefore, efficiency approaching 20% is realistically possible from a solid-state mesoscopic solar cell based on $\text{CH}_3\text{NH}_3\text{PbX}_3$. When comparing an organometal halide perovskite light absorber with metal chalcogenide quantum dots, the former exhibits better performance with a higher photovoltage, although perovskite and metal chalcogenide have similar absorption coefficients.⁶⁰ Thus, further systematic investigation of an organometal halide light absorber is required to understand its unique nature in light absorption and carrier conduction over existing quantum dots and organic sensitizers.

AUTHOR INFORMATION

Corresponding Author

*E-mail: npark@skku.edu. Tel: 82-31-290-7241. Fax: 82-31-290-7272

Notes

The authors declare no competing financial interest.

ACKNOWLEDGMENTS

This work was supported by the National Research Foundation of Korea (NRF) grants funded by the Ministry of Science, ICT & Future Planning (MSIP) of Korea under Contracts NRF-2010-0014992, NRF-2012M1A2A2671721, NRF-2012-M3A6A7054861 (Nano Material Technology Development Program), and NRF-2012M3A6A7054861 (Global Frontier R&D Program on Center for Multiscale Energy System).

REFERENCES

- O'Regan, B.; Grätzel, M. A Low-Cost, High-Efficiency Solar Cell Based on Dye-Sensitized Colloidal TiO_2 Films. *Nature* **1991**, *353*, 737–740.
- Yella, A.; Lee, H.-W.; Tsao, H. N.; Yi, C.; Chandiran, A. K.; Nazeeruddin, Md. K.; Diau, E. W.-G.; Yeh, C.-Y.; Zakeeruddin, S. M.; Grätzel, M. Porphyrin-Sensitized Solar Cells with Cobalt (II/III)-Based Redox Electrolyte Exceed 12% Efficiency. *Science* **2011**, *334*, 629–634.
- Bach, U.; Lupo, D.; Comte, P.; Moser, J. E.; Weissörtel, F.; Salbeck, J.; Spreitzer, H.; Grätzel, M. Solid-State Dye-Sensitized Mesoporous TiO_2 Solar Cells with High Photon-to-Electron Conversion Efficiency. *Nature* **1998**, *395*, 583–585.
- Krüger, J.; Plass, R.; Cevey, L.; Piccirelli, M.; Grätzel, M. High Efficiency Solid-State Photovoltaic Device Due to Inhibition of Interface Charge Recombination. *Appl. Phys. Lett.* **2001**, *79*, 2085–2087.
- Krüger, J.; Plass, R.; Grätzel, M.; Matthieu, H.-J. Improvement of the Photovoltaic Performance of Solid-State Dye-Sensitized Device by Silver Complexation of the Sensitizer cis-Bis(4,4'-dicarboxy-2,2'-bipyridine)-bis(isothiocyanato) Ruthenium (II). *Appl. Phys. Lett.* **2002**, *81*, 367–369.
- Schmidt-Mende, L.; Zakeeruddin, S. M.; Grätzel, M. Efficiency Improvement in Solid-State-Dye-Sensitized Photovoltaics with an Amphiphilic Ruthenium-Dye. *Appl. Phys. Lett.* **2005**, *86*, 013504.
- Schmidt-Mende, L.; Bach, U.; Humphry-Baker, R.; Horiuchi, T.; Miura, H.; Ito, S.; Uchida, S.; Grätzel, M. Organic Dye for Highly Efficient Solid-State Dye-Sensitized Solar Cells. *Adv. Mater.* **2005**, *17*, 813–815.
- Wang, M.; Moon, S.-J.; Xu, M.; Chittibabu, K.; Wang, P.; Cevey-Ha, N.-L.; Humphry-Baker, R.; Zakeeruddin, S. M.; Grätzel, M. Efficient and Stable Solid-State Dye-Sensitized Solar Cells Based on a High-Molar-Extinction-Coefficient Sensitizer. *Small* **2010**, *6*, 319–324.
- Cai, N.; Moon, S.-J.; Cevey-Ha, L.; Moehl, T.; Humphry-Baker, R.; Wang, P.; Zakeeruddin, S. M.; Grätzel, M. An Organic D- π -A Dye for Record Efficiency Solid-State Sensitized Heterojunction Solar Cells. *Nano Lett.* **2011**, *11*, 1452–1456.
- Snaith, H. J.; Grätzel, M. Enhanced Charge Mobility in a Molecular Hole Transporter via Addition of Redox Inactive Ionic Dopant: Implication to Dye-Sensitized Solar Cells. *Appl. Phys. Lett.* **2006**, *89*, 262114.
- Snaith, H. J.; Schmidt-Mende, L. Advances in Liquid-Electrolyte and Solid-State Dye-Sensitized Solar Cells. *Adv. Mater.* **2007**, *19*, 3187–3200.
- Burschka, J.; Dualeh, A.; Kessler, F.; Baranoff, E.; Cevey-Ha, N.-L.; Yi, C.; Nazeeruddin, M. K.; Grätzel, M. Tris(2-(1H-pyrazol-1-yl)pyridine)cobalt(III) as P-Type Dopant for Organic Semiconductors and Its Application in Highly Efficient Solid-State Dye-Sensitized Solar Cells. *J. Am. Chem. Soc.* **2011**, *133*, 18042–18045.
- Tan, S.; Zhai, J.; Wan, M.; Meng, Q.; Li, Y.; Jiang, L.; Zhu, D. Influence of Small Molecules in Conducting Polyaniline on the Photovoltaic Properties of Solid-State Dye-Sensitized Solar Cells. *J. Phys. Chem. B* **2004**, *108*, 18693–18697.
- Cervini, R.; Cheng, Y.; Simon, G. Solid-State Ru-Dye Solar Cells Using Polypyrrole As a Hole Conductor. *J. Phys. D: Appl. Phys.* **2004**, *37*, 13.
- Kudo, N.; Honda, S.; Shimazaki, Y.; Ohkita, H.; Ito, S. Improvement of Charge Injection Efficiency in Organic–Inorganic Hybrid Solar Cells by Chemical Modification of Metal Oxides with Organic Molecules. *Appl. Phys. Lett.* **2007**, *90*, 183513.
- Zafer, C.; Karapire, C.; Sariciftci, N. S.; Icli, S. Characterization of N,N'-Bis-2-(1-hydroxy-4-methylpentyl)-3,4,9,10-perylene bis (dicarboximide) Sensitized Nanocrystalline TiO_2 Solar Cells with Polythiophene Hole Conductors. *Sol. Energy Mater. Sol. Cells* **2005**, *88*, 11–21.
- Lancelle-Beltran, E.; Prené, P.; Boscher, C.; Belleville, P.; Buvat, P.; Lambert, S.; Guillet, F.; Marcel, C.; Sanchez, C. Solid-State Organic/Inorganic Hybrid Solar Cells Based on Poly(Octylthiophene) and Dye-Sensitized Nanobrookite and Nanoanatase TiO_2 Electrodes. *Eur. J. Inorg. Chem.* **2008**, 903–910.
- Coakley, K. M.; Liu, Y. X.; McGehee, M. D.; Frindell, K. L.; Stucky, G. D. Infiltrating Semiconducting Polymers into Self-

Assembled Mesoporous Titania Films for Photovoltaic Applications. *Adv. Funct. Mater.* **2003**, *13*, 301–306.

(19) Coakley, K. M.; McGehee, M. D. Photovoltaic Cells Made from Conjugated Polymers Infiltrated into Mesoporous Titania. *Appl. Phys. Lett.* **2003**, *83*, 3380–3382.

(20) Zhu, R.; Jiang, C. Y.; Liu, B.; Ramakrishna, S. Highly Efficient Nanoporous TiO₂-Polythiophene Hybrid Solar Cells Based on Interfacial Modification Using a Metal-Free Organic Dye. *Adv. Mater.* **2009**, *21*, 994–1000.

(21) Abrusci, A.; Kumar, R. S. S.; Al-Hashimi, M.; Heeney, M.; Petrozza, A.; Snaith, H. J. Influence of Ion Induced Local Coulomb Field and Polarity on Charge Generation and Efficiency in Poly(3-hexylthiophene)-Based Solid-State Dye-Sensitized Solar Cells. *Adv. Funct. Mater.* **2011**, *21*, 2571–2579.

(22) Mor, G. K.; Kim, S.; Paulose, M.; Varghese, O. K.; Shankar, K.; Basham, J.; Grimes, C. A. Visible to Near-Infrared Light Harvesting in TiO₂ Nanotube Array-P3HT Based Heterojunction Solar Cells. *Nano Lett.* **2009**, *9*, 4250–4257.

(23) Chang, J. A.; Rhee, J. H.; Im, S. H.; Lee, Y. H.; Kim, H.-j.; Seok, S. I.; Nazeeruddin, M. K.; Grätzel, M. High-Performance Nanostructured Inorganic–Organic Heterojunction Solar Cells. *Nano Lett.* **2010**, *10*, 2609–2612.

(24) Im, S. H.; Lim, C.-S.; Chang, J. A.; Lee, Y. H.; Maiti, N.; Kim, H.-J.; Nazeeruddin, M. K.; Grätzel, M.; Seok, S. I. Toward Interaction of Sensitizer and Functional Moieties in Hole-Transporting Materials for Efficient Semiconductor-Sensitized Solar Cells. *Nano Lett.* **2011**, *11*, 4789–4793.

(25) Chang, J. A.; Im, S. H.; Lee, Y. H.; Kim, H.-j.; Lim, C.-S.; Heo, J. H.; Seok, S. I. Panchromatic Photon-Harvesting by Hole-Conducting Materials in Inorganic–Organic Heterojunction Sensitized-Solar Cell through the Formation of Nanostructured Electron Channels. *Nano Lett.* **2012**, *12*, 1863–1867.

(26) Kim, H.-S.; Lee, C.-R.; Im, J.-H.; Lee, K.-B.; Moehl, T.; Marchioro, A.; Moon, S.-J.; Humphry-Baker, R.; Yum, J.-H.; Moser, J. E.; et al. Lead Iodide Perovskite Sensitized All-Solid-State Submicron Thin Film Mesoscopic Solar Cell with Efficiency Exceeding 9%. *Sci. Rep.* **2012**, *2*, 591.

(27) Lee, M. M.; Teuscher, J.; Miyasaka, T.; Murakami, T. N.; Snaith, H. J. Efficient Hybrid Solar Cells Based on Meso-Superstructured Organometal Halide Perovskites. *Science* **2012**, *338*, 643–647.

(28) Noh, J. H.; Im, S. H.; Heo, J. H.; Mandal, T. N.; Seok, S. I. Chemical Management for Colorful, Efficient, and Stable Inorganic–Organic Hybrid Nanostructured Solar Cells. *Nano Lett.* **2013**, *13*, 1764–1769.

(29) Snaith, H. J.; Humphry-Baker, R.; Chen, P.; Cesar, I.; Zakeeruddin, S. M.; Grätzel, M. Charge Collection and Pore Filling in Solid-State Dye-Sensitized Solar Cells. *Nanotechnol.* **2008**, *19*, 424003.

(30) Ding, I.-K.; Tétreault, N.; Brillet, J.; Hardin, B. E.; Smith, E. H.; Rosenthal, S. J.; Sauvage, F.; Grätzel, M.; McGehee, M. D. Pore-Filling of Spiro-OMeTAD in Solid-State Dye Sensitized Solar Cells: Quantification, Mechanism, and Consequences for Device Performance. *Adv. Funct. Mater.* **2009**, *19*, 2431–2436.

(31) Melas-Kyriazi, J.; Ding, I.-K.; Marchioro, A.; Punzi, A.; Hardin, B. E.; Burkhard, G. F.; Tétreault, N.; Grätzel, M.; Moser, J.-E.; McGehee, M. D. The Effect of Hole Transport Material Pore Filling on Photovoltaic Performance in Solid-State Dye-Sensitized Solar Cells. *Adv. Energy Mater.* **2011**, *1*, 407–414.

(32) Docampo, P.; Hey, A.; Guldin, S.; Gunning, R.; Steiner, U.; Snaith, H. J. Pore Filling of Spiro-Ometad in Solid-State Dye-Sensitized Solar Cells Determined via Optical Reflectometry. *Adv. Funct. Mater.* **2012**, *22*, S010–S019.

(33) Yoo, B.; Kim, K.-J.; Bang, S.-Y.; Ko, M. J.; Kim, K.; Park, N.-G. Chemically Deposited Blocking Layers on FTO Substrates: Effect of Precursor Concentration on Photovoltaic Performance of Dye-Sensitized Solar Cells. *J. Electroanal. Chem.* **2010**, *638*, 161–166.

(34) Peng, B.; Jungmann, G.; Jäger, C.; Haarer, D.; Schmidt, H.-W.; Thelakkat, M. Systematic Investigation of the Role of Compact TiO₂

Layer in Solid State Dye-Sensitized TiO₂ Solar Cells. *Coord. Chem. Rev.* **2004**, *248*, 1479–1489.

(35) Snaith, H. J.; Grätzel, M. The Role of A “Schottky Barrier” at an Electron-Collection Electrode in Solid-State Dye-Sensitized Solar Cells. *Adv. Mater.* **2006**, *18*, 1910–1914.

(36) Karthikeyan, C. S.; Thelakkat, M. Key Aspects of Individual Layers in Solid-State Dye-Sensitized Solar Cells and Novel Concepts to Improve Their Performance. *Inorg. Chim. Acta* **2008**, *361*, 635–655.

(37) Lellig, P.; Niedermeier, M. A.; Rawolle, M.; Meister, M.; Laquai, F.; Müller-Buschbaum, P.; Gutmann, J. S. Comparative Study of Conventional and Hybrid Blocking Layers for Solid-State Dye-Sensitized Solar Cells. *Phys. Chem. Chem. Phys.* **2012**, *14*, 1607–1613.

(38) Kim, H.-S.; Ko, S.-B.; Jang, I.-H.; Park, N.-G. Improvement of Mass Transport of the [Co(Bpy)₃]II/III Redox Couple by Controlling Nanostructure of TiO₂ Films in Dye-Sensitized Solar Cells. *Chem. Commun.* **2011**, *47*, 12637–12639.

(39) Crossland, E. J. W.; Kamperman, M.; Nedelcu, M.; Ducati, C.; Wiesner, U.; Smilgies, D.-M.; Toombes, G. E. S.; Hillmyer, M. A.; Ludwigs, S.; Steiner, U.; Snaith, H. J. A Bicontinuous Double Gyroid Hybrid Solar Cell. *Nano Lett.* **2009**, *9*, 2807–2812.

(40) Docampo, P.; Stefiik, M.; Guldin, S.; Gunning, R.; Yufa, N. A.; Cai, N.; Wang, P.; Steiner, U.; Wiesner, U.; Snaith, H. J. Triblock-Terpolymer-Directed Self-Assembly of Mesoporous TiO₂: High-Performance Photoanodes for Solid-State Dye-Sensitized Solar Cells. *Adv. Energy Mater.* **2012**, *2*, 676–682.

(41) Docampo, P.; Tiwana, P.; Sakai, N.; Miura, H.; Herz, L.; Murakami, T.; Snaith, H. J. Unraveling The Function of an MgO Interlayer in Both Electrolyte and Solid-State SnO₂ Based Dye-Sensitized Solar Cells. *J. Phys. Chem. C* **2012**, *116*, 22840–22846.

(42) Kamat, P. V. Quantum Dot Solar Cells. Semiconductor Nanocrystals as Light Harvesters. *J. Phys. Chem. C* **2008**, *112*, 18737–18753.

(43) Rühle, S.; Shalom, M.; Zaban, A. Quantum-Dot-Sensitized Solar Cells. *ChemPhysChem* **2010**, *11*, 2290–2304.

(44) William, Yu, W.; Qu, L.; Guo, W.; Peng, X. Experimental Determination of the Extinction Coefficient of CdTe, CdSe, and CdS Nanocrystals. *Chem. Mater.* **2003**, *15*, 2854–2860.

(45) Helen, M. Crystal Structure of Barium Titanate. *Nature* **1945**, *155*, 484–485.

(46) Cava, R. J.; Batlogg, B.; Espinosa, G. P.; Ramirez, A. P.; Krajewski, J. J.; Peck, W. F., Jr; Rupp, L. W., Jr; Copper, A. S. Superconductivity at 3.5 K in BaPb_{0.75}Sb_{0.25}O₃: Why Is T_c So Low? *Nature* **1989**, *339*, 291–293.

(47) Schilling, A.; Cantoni, M.; Guo, J. D.; Ott, H. R. Superconductivity above 130 K in the Hg–Ba–Ca–Cu–O System. *Nature* **1993**, *363*, 56–58.

(48) Bhalla, A. S.; Guo, R. Y.; Roy, R. The Perovskite Structure — A Review of Its Role in Ceramic Science and Technology. *Mater. Res. Innovations* **2000**, *4*, 3–26.

(49) Ishihara, T.; Takahashi, J.; Goto, T. Optical Properties Due to Electronic Transitions in Two-Dimensional Semiconductors (C_nH_{2n+1}NH₃)₂PbI₄. *Phys. Rev. B* **1990**, *42*, 11099–11107.

(50) Calabrese, J.; Jones, N. L.; Harlow, R. L.; Herron, N.; Thorn, D. L.; Wang, Y. Preparation and Characterization of Layered Lead Halide Compounds. *J. Am. Chem. Soc.* **1991**, *113*, 2328–2330.

(51) Kawamura, Y.; Mashiyama, H.; Hasebe, K. Structural Study on Cubic–Tetragonal Transition of CH₃NH₃PbI₃. *J. Phys. Soc. Jpn.* **2002**, *71*, 1694–1697.

(52) Billing, D. G.; Lemmerer, A. Inorganic–Organic Hybrid Materials Incorporating Primary Cyclic Ammonium Cations: The Lead Iodide Series. *CrystEngComm* **2007**, *9*, 236–244.

(53) Tanaka, K.; Takahashi, T.; Ban, T.; Kondo, T.; Uchida, K.; Miura, N. Comparative Study on the Excitons in Lead-Halide-Based Perovskitetype Crystals CH₃NH₃PbBr₃CH₃NH₃PbI₃. *Solid State Commun.* **2003**, *127*, 619–623.

(54) Kojima, A.; Teshima, K.; Shirai, Y.; Miyasaka, T. Organometal Halide Perovskites as Visible-Light Sensitizers for Photovoltaic Cells. *J. Am. Chem. Soc.* **2009**, *131*, 6050–6051.

(55) Im, J.-H.; Lee, C.-R.; Lee, J.-W.; Park, S.-W.; Park, N.-G. 6.5% Efficient Perovskite Quantum-Dot-Sensitized Solar Cell. *Nanoscale* **2011**, *3*, 4088–4093.

(56) Etgar, L.; Gao, P.; Xue, Z.; Peng, Q.; Chandiran, A. K.; Liu, B.; Nazeeruddin, M. K.; Grätzel, M. Mesoscopic $\text{CH}_3\text{NH}_3\text{PbI}_3/\text{TiO}_2$ Heterojunction Solar Cells. *J. Am. Chem. Soc.* **2012**, *134*, 17396–17399.

(57) Edri, E.; Kirmayer, S.; Cahen, D.; Hodes, G. High Open-Circuit Voltage Solar Cells Based on Organic–Inorganic Lead Bromide Perovskite. *J. Phys. Chem. Lett.* **2013**, *4*, 897–902.

(58) Kamat, P. V. Quantum Dot Solar Cells. The Next Big Thing in Photovoltaics. *J. Phys. Chem. Lett.* **2013**, *4*, 908–918.

(59) Editorial. Reporting Solar Cell Efficiencies in Solar Energy Materials and Solar Cells. *Sol. Energy Mater. Sol. Cells* **2008**, *92*, 371–373.

(60) Miyasaka, T. Toward Printable Sensitized Mesoscopic Solar Cells: Light-Harvesting Management with Thin TiO_2 Films. *J. Phys. Chem. Lett.* **2011**, *2*, 262–269.